Multi-Techno-Band Cellular Network Resilience to Shocks and Aging: a Stochastic Geometry Approach

Ludmila Courtillat--Piazza
LTCI, Telecom Paris,
Institut Polytechnique de Paris
Palaiseau, France
lpiazza@telecom-paris.fr

Marceau Coupechoux
LTCI, Telecom Paris,
Institut Polytechnique de Paris
Palaiseau, France
coupecho@telecom-paris.fr

Sophie Quinton
Univ. Grenoble Alpes, INRIA,
CNRS, Grenoble INP, LIG
Grenoble, France
sophie.quinton@inria.fr

***Abstract*—While the resilience of networks facing disasters or brutal disturbances has emerged as a priority recently, especially since the COVID-19 pandemic, network resilience to continuous phenomena on a larger time scale still receive little attention. Yet, modeling and assessing the cumulative effect of long-term wear on a network would represent a key ingredient for understanding and planning network evolution. This article introduces a mobile network model allowing multiple technologies and bands (multi-TB) at a single base station (BS) based on stochastic geometry, and studies the resilience of such a network in front of shocks, or of its own aging process. Resilience metrics based on Signal to Interference plus Noise Ratio (SINR) and user data rate coverage probabilities are introduced and derived analytically. Numerical experiments show the influence of parameters such as load, BS density and the number of TB on network resilience.**

***Index Terms*—Resilience, stochastic geometry, cellular network, multi-techno-band**

I. Introduction

The COVID-19 pandemic and effects of global warming have recently raised the attention of authorities on our dependency to networks and the urgent need to study and increase their resilience. The resilience of mobile networks, defined as *the ability of the network to provide and maintain an acceptable level of service in the face of various faults and challenges to normal operation* [1], has been studied in the literature in the context of shocks such as natural disasters [2] or random disturbances [3], [4]. There has been however no research so far on the potential consequences on the network performance of possible long term and continuous disruptions in a changing and uncertain world. Semiconductor resources may for example become scarce, possibly due to shortages of raw material or environmental policy constraints. We thus argue the relevance of studying the resilience of mobile networks in the face of hardware aging. In this paper, we approach mobile network resilience using the stochastic geometry framework, propose a network model including multiple dependent techno-bands (TB) and derive approximate closed-form expressions for new resilience metrics.

While stochastic geometry is a wildly used framework for the study of statistical properties of mobile networks, to the best of our knowledge it has not been used for assessing the resilience of a mobile network facing disruptions. Existing work generally focuses on ad hoc solutions to face a disaster, for example deploying unmanned aerial vehicles [2]. Interestingly, metrics measuring the resilience of mobile networks were introduced in [4] and in [3]. However, in contrast to the present study they are not based on stochastic geometry. Work [3] focuses on short term disturbances but does not take into account the effect of continuous long term degradation of the network. Reference [4] adopts a deterministic geometric approach that does not take into account radio propagation and its influence on the quality of service (QoS). It introduces and applies resilience metrics on networks with different age configurations among BS but does not integrate the timing aspect in the resilience metric itself.

While multi-tier cellular networks are often studied in the literature, see e.g. [5], [6], multi-techno-bands (multi-TB) networks have not been modeled so far using stochastic geometry, to the best of our knowledge. In today's real-life mobile networks, multiple technologies and bands are indeed deployed at every BS. Contrary to multi-tier architectures, where small cells independently underlay a macro-cell network, TB are deployed at the same BS and are not independent from each other (for example 5G Non Stand Alone does depend on 4G) [7]. Deploying multiple TB at a BS also allows for *carrier aggregation*, i.e., the possibility for the user to increase its data rate. This characteristic of today's networks is thus crucial in terms of resilience.

The main contributions of this paper are:

- a multi-techno-band network model and its associated QoS metrics, namely Signal to Interference plus Noise Ratio (SINR) and user data rate coverage probabilities in a multi-TB network with carrier aggregation;
- a model for shocks and BS aging respectively based on the thinning and the continuous thinning of the BS point process and metrics for quantifying network resilience with respect to shocks and aging in the context of stochastic geometry;
- approximate closed-form formulas for coverage probabilities and resilience metrics in multi-TB networks;
- numerical results that validate our analytical results and show the impact of various parameters on network resilience.

The work of L. Courtillat–Piazza and M. Coupechoux has been performed at the LINCS laboratory (lincs.fr).

II. Network model

A. A multi-techno-band model

We consider the downlink of a cellular network made of a set of BS and a set of user equipment (UE). Every UE is served by the nearest BS. BS are likely to use multiple combinations of technologies (e.g. 4G, 5G) and frequency bands (e.g. 800 MHz, 3.5 GHz). A TB b is characterized by a technology, a carrier frequency f_b and a bandwidth W_b. We assume that two TB do not interfere at the UE, as they use orthogonal spectrum resources. Every UE is supposed to be able to connect to any TB of its serving BS and to aggregate the data rates of the different available TB thanks to the *carrier aggregation* technique. We assume that there is a dependence relation between TB deployed at a BS, which holds whenever a given TB cannot be deployed at a BS unless another TB is already deployed at this BS. This dependence can be required (e.g. a 5G Non Stand Alone BS shall be deployed in conjunction with 4G), or chosen by an operator.

The multi-TB network model is defined as follows. Let $\mathscr{B}$ be the set of all TB present in the network. Let $<_{\mathscr{B}}$ be a total ordering relation on the TB, related to the chronology of their deployment. Let $D(.)$ be a function which maps a TB to the set of TB it requires to be deployed on a BS. We assume that a TB cannot depend on a TB of higher generation, i.e.:

$$\forall b_1, b_2 \in \mathscr{B} \quad b_1 \in D(b_2) \quad \Rightarrow \quad b_1 <_{\mathscr{B}} b_2 \tag{1}$$

Let $\mathcal{B} \subseteq P(\mathscr{B})$ be the set of all sets of TB that can be present together at a same BS as they respect the dependency relation between TB expressed by D. Hence, $\mathcal{B}$ is the set of all subsets B of $\mathscr{B}$ such that for any $b_1 \in B$, all b_2 in $D(b_1)$ are also in B. The set of TB present at BS i is denoted by B_i.

The deployment of the multi-TB network is performed as follows. For each BS i, each TB b is iteratively considered for deployment following the total ordering $<_{\mathscr{B}}$. TB b is associated with a probability p_b of being deployed at BS i if all TB in $D(b)$ are already deployed at i, and with a probability 0 otherwise:

$$\mathbb{P}(b \in B_i) = \begin{cases} p_b & \text{if } D(b) \subseteq B_i(b) \\ 0 & \text{else} \end{cases} \tag{2}$$

where $B_i(b)$ is the partial set of B_i at the time when TB b is to be deployed. In addition, the constraint $p_{b_1} = 1$ holds for the TB of minimal rank $b_1 = \{b \mid \forall b' \in \mathscr{B} \setminus \{b\}, b <_{\mathscr{B}} b'\}$. Thus, all BS have at least one TB.

B. Stochastic geometry model

BS locations are modeled by a homogeneous Poisson Point Process (PPP) Φ_{BS} of intensity λ_{BS}. The set of TB present at each BS is assigned by applying a marking operation $\mathbf{m}(\cdot)$ on PPP Φ_{BS}. The marking operation $\mathbf{m}(\cdot)$ is defined by its set of marks $\mathcal{B}$ and the distribution of each mark. The probability of a mark $B \in \mathcal{B}$ corresponds to the probability of B being the set of TB present on a given BS. It is provided in Sec. V-A. Thus, every BS of the marked process $\mathbf{m}(\Phi_{BS})$ is associated with a random mark B which is the set of its TB. For a TB $b \in \mathscr{B}$, $\mathbf{m}_b(\Phi_{BS})$ denotes the set of BS of $\mathbf{m}(\Phi_{BS})$ with TB b in their mark. It is the PPP induced by the union of marks in $\mathcal{B}$ including b. Its intensity is given by $\lambda_{BS,b} = (p_b \prod_{b' \in D(b)} p_{b'})\lambda_{BS}$.

UE positions are modeled by a homogeneous PPP Φ_{UE} of intensity λ_{UE}. In addition, we note $k_{avg} = \lambda_{UE}/\lambda_{BS}$.

C. Shocks and aging models

We define a *shock* with probability p as an event that suddenly renders a proportion s of BS unusable. A shock on the network is represented by an independent p-thinning $\mathbf{t}_p(\cdot)$ of parameter p applied to PPP Φ_{BS}. Parameter p is the proportion of BS failing due to this shock.

The *aging* of the network is modeled by applying a *continuous thinning* $\mathbf{t}_{p(t)}(\cdot)$ of parameter $p(t)$ on Φ_{BS}. We call *continuous thinning* an independent p-thinning of parameter p applied on a PPP, such that p depends on time t. That is, at time t, each point of Φ_{BS} has a probability $p(t)$ of remaining alive. The proportion $p(t)$ represents the cumulative distribution function (cdf) of the lifetime of any BS starting at time 0. To model this lifetime cdf, we introduce two random variables (r.v.): T, the total lifetime of a BS, and T_0 the age of a BS at $t = 0$, so that: $p(t) = \mathbb{P}(t + T_0 < T)$. Assuming that T follows a Weibull law of parameters (α, β) and T_0 follows a uniform law on $[0, T]$:

$$p(t) = e^{-\left(\frac{t}{\alpha}\right)^{\beta}} - \frac{t}{\alpha} \int_{v=\left(\frac{t}{\alpha}\right)^{\beta}}^{+\infty} v^{-\frac{1}{\beta}} e^{-v} \, dv \tag{3}$$

The use of a Weibull law is motivated by previous work on failure laws for wireless communication hardware systems [8].

III. QoS metrics

SINR and user data rate coverage probabilities are used as QoS metrics. If $q(\cdot)$ designates either SINR or user data rate and Γ is a threshold, the coverage probability is defined as: $cp(q, \Gamma) = \mathbb{P}(q(u) > \Gamma)$. We will focus on small values of Γ as our objective is to ensure a minimal service in the context of network degradation. In the following, u is an arbitrary point of $\mathbb{R}^2$ and $i(u)$ (denoted i by abuse of notation) is the point in Φ_{BS} that is nearest to u .

A. SINR coverage probabilities

1) Mono-TB SINR coverage probability: The (Signal to Interference plus Noise Ratio) SINR related to a single TB b is given by:

$$\gamma_b(u) = \frac{P_{i \to u,b}}{I_{iub} + \sigma_b^2} \tag{4}$$

where $P_{i \to u,b}$ and I_{iub} are respectively the useful power received by u from i and the interference received by u from BS other than i in TB b, and σ_b^2 is the thermal noise power in TB b. The useful received power is given by:

$$P_{i \to u,b} = G_b P_b h_{iub} \kappa_b d(i,u)^{-\eta_b} \tag{5}$$

where G_b is the BS antenna gain, P_b is the BS output power, h_{iub} is the fast fading coefficient between u and i on b, $d(i,u)$ is the distance between u and its serving BS and (κ_b, η_b) are path-loss parameters. The BS antenna gain is supposed to be

constant which reflects the adaptative directivity of the signal from the BS to the attached UE. Fast fading coefficients are modeled with independent and identically distributed exponential r.v. of parameter μ. The interference I_{iub} is given by:

$$I_{iub} = \sum_{j \in \mathbf{m}_b(\Phi_{BS}),\ j \neq i} P_{j \to u,b} \tag{6}$$

were $P_{j \to u,b}$ is expressed by (5) in which G_b is replaced by G'_b which is the antenna gain of interfering BS in the direction of u. Note that only BS with TB b interfere with i at u on b. Hence the sum in (6) is on the elements of the process $\mathbf{m}_b(\Phi_{BS})$ induced by mark b on Φ_{BS}. The thermal noise power is given by $\sigma_b^2 = N_0 W_b N_f$, where N_0 is the thermal noise power spectral density, W_b is the bandwidth of b and N_f is a noise factor at the UE.

2) Multi-TB SINR coverage probability: In a multi-TB network, a user can connect to any of the available TB deployed at its serving BS. It is said to be *covered* if at least one TB provides the required quality. As a consequence, the coverage probability related to multi-TB SINR γ is defined as the probability of the SINR γ_b associated with *any* TB of the cell of u being greater than Γ_γ, that is:

$$cp(\gamma, \Gamma_\gamma) = \mathbb{P}\left(\bigcup_{b \in B_i} \{\gamma_b(u) > \Gamma_\gamma\} \right) \tag{7}$$

B. User data rate coverage probabilities

1) Mono-TB user data rate: Considering co-channel interference as noise, the Shannon formula can be applied to approximate the *physical data rate* at u on TB b: $C_b(u) = W_b \log_2(1 + \gamma_b(u))$. Assuming an equal share of resources between users, the *user data rate* is now obtained as $\tilde{C}_b(u) = \frac{1}{k_i} C_b(u)$, where $k_i \geq 1$ is the number of users in cell i.

2) Multi-TB user data rate: In a multi-TB network with carrier aggregation, the physical data rate $C(u)$ available in the cell of BS i is the sum of the data rates $C_b(u)$ provided by all the TB b deployed in this cell. The user data rate $\tilde{C}(u)$ is thus given by $\tilde{C}(u) = \frac{1}{k_i} \sum_{b \in B_i} C_b(u)$ and associated coverage probability is given by:

$$cp(\tilde{C}, \Gamma_C) = \mathbb{P}\left(\frac{1}{k_i} \sum_{b \in B_i} C_b(u) > \Gamma_C \right) \tag{8}$$

IV. Resilience metrics

A. Resilience to shocks

We introduce a resilience metric for a mobile network facing shocks, defined as the proportion of the QoS that is maintained when each BS becomes unusable with probability s, that is when thinning $\mathbf{t}_p(\cdot)$ is applied on Φ_{BS} with $p = 1 - s$:

$$R^s_\Gamma(s) = \frac{\mathbb{P}(q(u) > \Gamma,\ p = 1 - s)}{\mathbb{P}(q(u) > \Gamma,\ p = 1)} \tag{9}$$

This metric is inspired by the literature and adapted to the stochastic geometry framework. In particular, [4] also introduced a resilience metric which is a proportion of network area remaining covered. Coverage is there measured based on geometrical computation on cells with fixed maximum radius, in contrast to our metric taking in account radio propagation effects and a coverage based on the quality of received signal.

B. Resilience to aging

We now extend the previous metric to a temporal metric measuring resilience as the proportion of the QoS that is maintained as BS become unusable over time:

$$R^a_\Gamma(\Delta t) = \frac{\mathbb{P}(q(u) > \Gamma,\ t = t_0 + \Delta t)}{\mathbb{P}(q(u) > \Gamma,\ t = t_0)} \tag{10}$$

Defining resilience as the ratio between a QoS metric *after* and *before* a disturbance can be found in the literature, see [9]. Note that (10) extends (9) if t_0 is the time instant of the shock and Δt is small. Note also that the present metric applies on a long term time scale contrary to the previous ones in literature.

V. Analytical Results

A. Marks distribution

The probability of any $B \in \mathcal{B}$ being the set of TB present at a given BS is provided by:

$$\forall B \in \mathcal{B},\ \mathbb{P}(B_i = B) = \prod_{b \in B} p_b \left(\prod_{b \notin B,\ D(b) \subseteq B} (1 - p_b) \right) \tag{11}$$

B. Mono-TB SINR coverage probability

The expression of coverage probability related to mono-TB-SINR is given by [10]:

$$cp(\gamma_b, \Gamma_\gamma) = \int_{r>0} f_{R_0,b}(r) \mathscr{N}_b(r, \Gamma_\gamma) \mathscr{I}_b(r, \Gamma_\gamma)\ dr \tag{12}$$

where $f_{R_0,b}(r)$ is the cdf of the distance between u and its nearest point i of Φ_{BS} with TB b, $\mathscr{N}_b$ is the thermal-noise-related term and $\mathscr{I}_b$ is the interference-related term. Note that (12) is expressed as a conditioning on distance $d(i,u)$ where $\mathscr{N}_b(r, \Gamma_\gamma)\mathscr{I}_b(r, \Gamma_\gamma) = cp(\gamma_b, \Gamma_\gamma \mid r) = \mathbb{P}(\gamma_b(u) > \Gamma_\gamma \mid r)$. The cdf of the distance between u and i is given by:

$$f_{R_0,b}(r) = 2\lambda_{BS,b} \pi r e^{-\lambda_{BS,b} \pi r^2} \tag{13}$$

The thermal-noise-related term is given by:

$$\mathscr{N}_b(r, \Gamma_\gamma) = \exp\left(-\frac{\mu \Gamma_\gamma \sigma_b^2}{G_b P_b \kappa_b r^{-\eta_b}} \right) \tag{14}$$

With $a = \left(\frac{\Gamma_\gamma G'_b}{G_b} \right)$, the interference-related term is given by:

$$\mathscr{I}_b(r, \Gamma) = \exp\left(-\pi \lambda_{BS,b} r^2 a^{\frac{2}{\eta_b}} \int_{a^{-\frac{2}{\eta_b}}}^{+\infty} \frac{1}{z^{\frac{\eta_b}{2}} + 1}\ dz \right) \tag{15}$$

C. Multi-TB SINR coverage probability

The multi-TB SINR coverage probability defined in (7) can be written as follows, by conditioning on distance $d(i,u)$:

$$cp(\gamma, \Gamma_\gamma) = \int_{r>0} \mathbb{P}\left(\bigcup_{b \in B_i} \{\gamma_b(u) > \Gamma_\gamma\} \middle| r \right) f_{R_0}(r)\ dr \tag{16}$$

where $f_{R_0}(r) = 2\lambda_{BS} \pi r e^{-\lambda_{BS} \pi r^2}$ is the cdf of the distance between u and i its nearest point of Φ_{BS}. Regarding the

conditional probability, by replacing $\gamma_b(u)$ by its expression, applying the De Morgan law and expressing the partial expectation at B_i, (17) is derived. With the approximation that the I_{iub} are independent, (18) holds.

$$\mathbb{P}\left(\bigcup_{b\in B_i}\{\gamma(u,b)>\Gamma_\gamma\}\middle| r\right)$$
$$=1-\mathbb{E}_{[B_i]}\left[\mathbb{P}\left(\bigcap_{b\in B_i}\left\{\frac{G_bP_bh_{iub}\kappa_b r^{\eta_b}}{I_{iub}+\sigma_b^2}\leq\Gamma_\gamma\right\}\middle| r\right)\right] \quad (17)$$
$$\sim 1-\sum_{B\in\mathcal{B}}\mathbb{P}(B_i=B)\prod_{b\in B}\mathbb{P}\left(\frac{G_bP_bh_{iub}\kappa_b r^{\eta_b}}{I_{iub}+\sigma_b^2}\leq\Gamma_\gamma\middle| r\right) \quad (18)$$

Each term in the product in (18) is the complementary probability of a mono-TB coverage probability $pc(\gamma_b,\Gamma_\gamma \mid r)$ conditioned on r, i.e.:

$$\mathbb{P}\left(\frac{G_bP_bh_{iub}\kappa_b r^{\eta_b}}{I_{iub}+\sigma_b^2}\leq\Gamma_\gamma\middle| r\right)=1-\mathscr{N}_b(r,\Gamma_\gamma)\mathscr{I}_b(r,\Gamma_\gamma) \quad (19)$$

The final expression of the coverage probability is thus obtained by combining (16), (18), (19), (14), (15) and (13).

D. Mono-TB user data rate coverage probability

The mono-TB user data rate coverage probability can be easily deduced from the mono-TB SINR coverage probability as follows:

$$cp(\tilde{C}_b,\Gamma_C)=\mathbb{P}\left(\gamma_b(u)>2^{\frac{k_i}{W}\Gamma_C}-1\right) \quad (20)$$

Note that in this expression, k_i is a r.v. The derivation of the distribution of k_i requires the expression of the distribution of Voronoi cell areas produced by a PPP, which is still an open problem to the best of our knowledge [11]. Hence, k_i is approximated by its average value: $k^*_{avg}=\mathbb{E}(k_i|k_i>0)=\frac{\lambda_{UE}/\lambda_{BS}}{1-e^{-\lambda_{UE}/\lambda_{BS}}}$.

E. Multi-TB user data rate coverage probability

Equation (8) expresses the multi-TB user data rate coverage probability. By replacing $\tilde{C}_b(u)$ by its expression we obtain:

$$cp(\tilde{C},\Gamma_C)=\mathbb{P}\left(\frac{1}{k_i}\sum_{b\in B_i}W_b\log_2(\gamma_b(u)+1)>\Gamma_C\right) \quad (21)$$

Approximating $\log_2(x+1)$ by x when x is small, we have:

$$cp(\tilde{C},\Gamma_C)\sim\mathbb{P}\left(\sum_{b\in B_i}W_b\gamma_b(u)>k_i\Gamma_C\right) \quad (22)$$

With $\Gamma^*_C=k_i\Gamma_C$, by computing partial expectation at B_i:

$$cp(\tilde{C},\Gamma_C)\sim\sum_{B\in\mathcal{B}}\mathbb{P}(B_i=B)\mathbb{P}\left(\sum_{b\in B}W_b\gamma_b(u)>\Gamma^*_C\right) \quad (23)$$

For a fixed B_i, we note $B_i=\{b_1,\ldots,b_m\}$ with $b_1<_{\mathscr{B}}b_2<_{\mathscr{B}}\cdots<_{\mathscr{B}}b_m$. We can then introduce successively the conditional expectation on each of the BS except b_1. The probability density function of the SINR associated to TB b is denoted by $f_{\gamma_b}(v)$. Assuming here that TB are independent, (24) holds. The expression of $f_{\gamma_b}(v)$ is obtained by derivation of (12) and provided by (25).

	Antenna & signal parameters	
	Default urban (UMa)	Rural (RMa)
Notation	Value	
P_b	46 dBm	
G_b, G'_b	17 dBi	
μ	1	
N_0	-174 dBm/Hz	
N_f	8 dB	
(η_1,κ_1)	(3.91, 0.0692)	(3.86, 0.677)
(η_2,κ_2)	(3.91 0.00655)	(3.86, 0.0641)
(η_3,κ_3)	(3.91 0.0903)	(3.86, 0.884)
d_{avg}	700 m	2500 m
k_{avg}	5	

Techno-bands				
Rank ($<_{\mathscr{B}}$)	Generation	f_b (MHz)	W (MHz)	$D(.)$
1 (Default)	4G	800	23.74	/
2 (Default)	4G	1800	51.25	{1}
3	5G	900	23.74	{1}

TABLE I: Parameters.

F. Shock and aging influence on probabilities

Shocks and aging only influence the BS density. All previous equations remain valid after a shock s or after a duration Δt if λ_{BS} is replaced by its thinned equivalent. In case of a shock s, λ_{BS} is replaced by $p\lambda_{BS}$ with $p=1-s$. In case of aging, it is replaced by $\lambda_{BS}(t)$ with $\lambda_{BS}(t)=p(t)\lambda_{BS}$. The thinning parameter expression $p(t)$ was provided by (3).

VI. Numerical Results

A. Simulation settings

Simulation parameters are shown in Tab. I. TB are identified by their rank. Unless specified, default parameters are for a urban environment, two TB with probabilities $[p_1=1,p_2=0.7]$, a SINR threshold of $\Gamma_\gamma=-2$ dB and a data rate threshold of $\Gamma_C=0.5$ Mbps. Path-loss parameters (κ_b,η_b) are derived from the 3GPP UMa ($PL'_{UMa-NLOS}$) and RMa ($PL'_{RMa-NLOS}$) models [12] and are given for every TB. In addition, for 3.5 GHz, $\kappa_b=0.00361$ and $\eta_b=3.91$ in a urban environment. The BS density λ_{BS} is derived from the average inter-BS distance d_{avg}. Weibull parameters are $\alpha=8.3606$ and $\beta=3.3035$, which translate to an expected lifetime of 7.5 years at birth [4], and 3.75 years in our experiments.

B. Validity of approximations

Fig. 1 allows comparison of the user data rate coverage probability approximated with our analytical results and estimated with Monte-Carlo simulations (10.000 iterations). The most impacting approximation is on $\log(1+x)$ when Γ_C is increasing but recall that we are targeting low data rates allowing to access basic services. This approximation causes the proposed formulas to be less precise when k^*_{avg} is higher, as the number of users multiplies Γ_C in the user data rate coverage probability. The TB's independence assumption is less impacting when p_2 is close to 0.5. The approximation on the distribution of k_i is less impacting when k^*_{avg} is higher because of the law of large numbers. Despite these approximations, we see that analytical results match pretty well the simulations as long as parameters Γ_C and k^*_{avg} are not too high. We now present only analytical results.

$$\mathbb{P}\left(\sum_{b\in B} W_b\gamma_b(u) > \Gamma_C^*\right) = \int_{v_2=0}^{+\infty}\cdots\int_{v_m=0}^{+\infty}\mathbb{P}\left(\left\{\gamma_{b_1}(u) > \frac{1}{W_{b_1}}\left(\Gamma_C^* - \sum_{l\in[\![2,m]\!]} W_l v_l\right)\right\}\right) \times \prod_{l\in[\![2,m]\!]} f_{\gamma_{b_l}}(v_l)\; dv_2 \ldots dv_m \quad (24)$$

$$f_{\gamma_b}(v) = \int_{r>0} f_{R_0}(r)\mathcal{N}_b(r,v)\mathcal{I}_b(r,v)\left[\frac{\mu\sigma_b^2}{G_b P_b \kappa_b r^{-\eta_b}} + \frac{2\pi\lambda_{BS,b} r^2}{\eta_b}\left[\frac{G_b'}{G_b + G_b' v} + \frac{1}{v}\left(\frac{G_b' v}{G_b}\right)^{\frac{2}{\eta_b}} \int_{\left(\frac{G_b' v}{G_b}\right)^{-\frac{2}{\eta_b}}}^{+\infty} \frac{1}{z^{\frac{\eta_b}{2}} + 1}\; dz\right]\right] dr \quad (25)$$

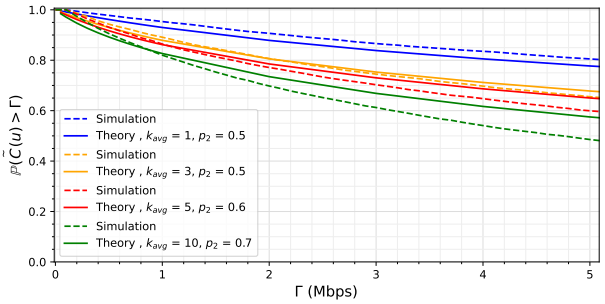

Fig. 1: Simulation vs. analysis for the user data rate coverage probability.

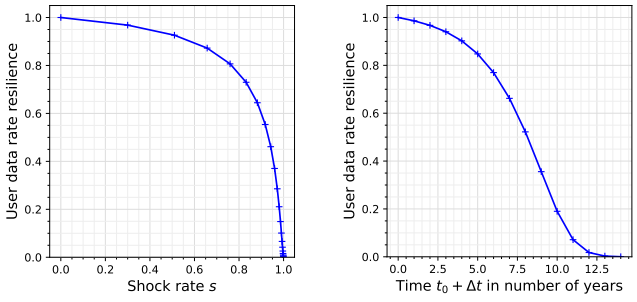

(a) (b)

Fig. 2: User data rate resilience to shocks (a) and to aging (b).

C. Resilience to shock VS resilience to aging

Fig. 2 compares the network resilience in terms of shocks (a) and in terms of aging (b). Recall that the resilience to shocks expresses the loss of QoS for a given proportion of randomly failing BS, while the resilience to aging expresses the cumulative effect of BS failing at the end of their life. In our scenario, the network is resilient to shocks of very high amplitude, e.g., resilience is above 0.8 for shocks involving the destruction of less than 75% of BS. On the other hand, resilience to aging falls below 0.8 after 5.25 years. While the literature has up to now focused on shocks metrics, resilience to aging captures a cumulative effect and a temporal dynamics. This allows for a predictive tool for planning.

D. Impact of various parameters on resilience to aging

We study here the influence of some network parameters and design choices on resilience to aging. We focus on the user data rate resilience, but conclusions are similar for the SINR resilience in this section. A lower coverage threshold Γ significantly increases resilience, see Fig. 3a, as the network is able to serve a higher number of users with the required quality. In the same way, fewer UE per BS, see Fig. 3b, allows the network to dedicate more resources per user and can thus better absorb BS losses. When the inter-BS distance is smaller, resilience increases, see Fig. 3c, because of a higher overlapping in terms of radio coverage. To study the influence of the carrier frequency, we focus on a single-TB scenario and consider the SINR resilience to get rid of the influence of the bandwidth, see Fig. 3d. The lower the carrier frequency is, the better the radio propagation, which in turn implies a higher overlapping of radio coverage between cells. When BS are failing, momentarily disconnected users can hence be more easily served by neighboring cells. Lower frequencies thus lead to a higher resilience. The comparison between urban and rural environment shows the conflicting effects of several network parameters, see Fig. 4. Rural environments benefit from favorable radio propagation conditions, which tends to increase the resilience. However, this also comes usually with higher inter-BS distances because of a lower load. This effect tends to decrease resilience. On the contrary, urban networks are designed to sustain a high capacity and cells are thus smaller. In our scenario, this effect is predominant and leads to a better resilience of the urban network. The conclusion cannot be generalized but illustrates the importance of defining various resilience metrics.

E. Multi-TB network and resilience

The influence of the number of TB on resilience to aging is illustrated in Fig. 5. A remarkable result is that the effect of the number of TB on SINR and user data rate resilience is different. Regarding SINR resilience to aging, the dominant effect can be explained by the conjunction of frequency diversity and the lack of resilience of high carrier frequency. Indeed, at time t_0, the 2-TB network offers a much better QoS than the 1-TB network because of its two frequency bands that bring users diversity in frequency. The 3-TB network offers an even higher QoS. The denominator of (10) is thus higher when the number of TB is higher. Over time, however, degradation is steeper for TB 2, which is a high-frequency TB. Then, the 2-TB network loses the benefit of frequency diversity because only a small part of it is now covered by the high frequency TB (TB 2). This explains a lower SINR resilience. TB 3's low

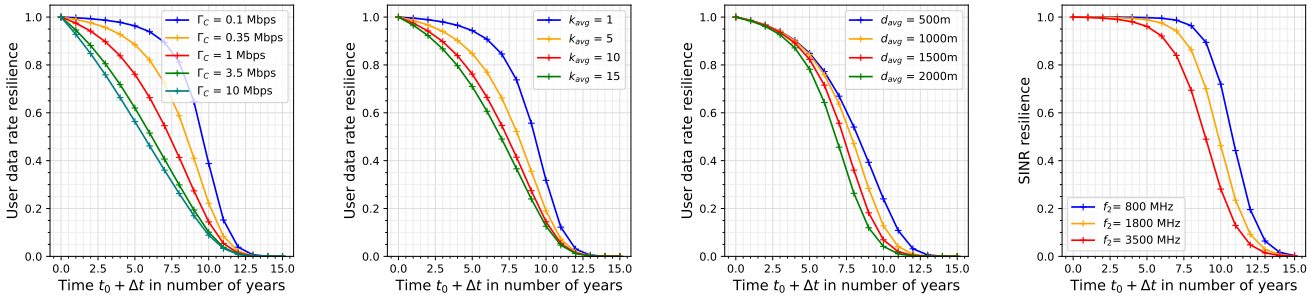

(a) (b) (c) (d)

Fig. 3: Influence of the coverage threshold Γ (a), the average number of UE per cell k_{avg} (b), the average inter-BS distance d_{avg} (c), the carrier frequency f_b (d) on resilience.

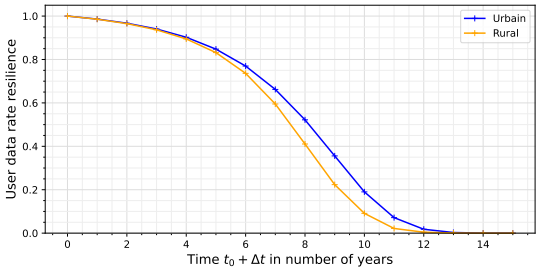

Fig. 4: Urban and rural networks resilience to aging.

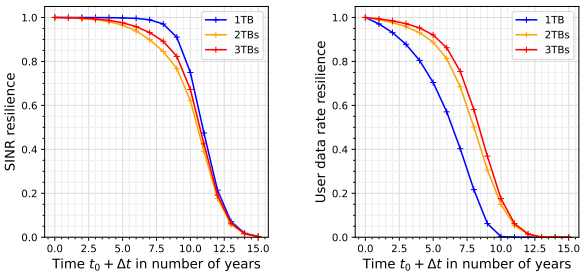

(a) (b)

Fig. 5: SINR (a) and user data rate (b) resilience to aging in function of the number of TB.

frequency allows partially keeping initial frequency diversity in the 3-TB network. When considering now the user data rate resilience, this effect is compensated by the gain that carrier aggregation brings by allowing the data rate of all TB to be used simultaneously, making the network with more TB the most resilient. This result illustrates the need to take into account the multiple TB of a network and different resilience metrics if recovery strategies should be deployed.

VII. Conclusion

We study the resilience of multi-techno-band cellular networks to shocks and BS aging using the stochastic geometry framework. We first propose a model for multi-techno-band networks that accounts for the dependencies between technologies and bands and derive SINR and user data rate coverage probabilities approximate closed-form formulas for these networks. We then propose resilience metrics related to SINR and user data rate that take into account both sudden disturbances, called shocks, and the temporal dynamics of a continuous degradation of the network due to BS aging. These resilience metrics are derived by modeling shocks as a thinning, and aging as a continuous thinning of the BS point process. Numerical experiments show the determining influence of the carrier frequency, the network load, the BS density, the coverage threshold and the number of techno-bands on resilience. With typical parameters, urban networks are shown to be more resilient than rural networks. The proposed model and analytical study pave the way for resilience estimations of real deployments and for adaptation strategies.

References

[1] J.P. Sterbenz et al., "Resilience and survivability in communication networks: Strategies, principles, and survey of disciplines."

[2] M. Matracia, M. A. Kishk, and M.-S. Alouini, "UAV-aided post-disaster cellular networks: A novel stochastic geometry approach," *IEEE Trans. Veh. Technol.*, vol. 72, no. 7, pp. 9406–9418, 2023.

[3] R.-J. Reifert, S. Roth, A. A. Ahmad, and A. Sezgin, "Comeback kid: Resilience for mixed-critical wireless network resource management," *IEEE Trans. Veh. Tech.*, vol. 72, no. 12, pp. 16 177–16 194, Dec. 2023.

[4] Z. Liang and Y.-F. Li, "Holistic resilience and reliability measures for cellular telecommunication networks," *Reliability Engineering & System Safety*, vol. 237, no. 109335, pp. 1–14, 9 2023.

[5] M. D. Renzo, "Stochastic geometry modeling and analysis of multi-tier millimeter wave cellular networks," *IEEE Trans. Wireless Commun.*, vol. 14, pp. 5038–5057, 10 2014.

[6] X. Tang, X. Xu, and M. Haenggi, "Meta distribution of the SIR in moving networks," *IEEE Trans. Commun.*, vol. 68, pp. 3614–3626, 6 2020.

[7] I. Buquicchio et al., "Energy and climate: lean networks for resilient connected uses - Appendix 1 (fr)," The Shift Project, Tech. Rep., 2023.

[8] J. Sun et al., "Research on reliability analysis method of wireless communication hardware system," in *Int. Conf. Computer Vision, Image and Deep Learning & Int. Conf. on Computer Engineering and Applications (CVIDL & ICCEA)*, May 2022, pp. 479–483.

[9] S. Hosseini, K. Barker, and J. E. Ramirez-Marquez, "A review of definitions and measures of system resilience," *Reliability Engineering & System Safety*, vol. 145, pp. 47–61, 2016.

[10] J. G. Andrews, F. Baccelli, and R. K. Ganti, "A tractable approach to coverage and rate in cellular networks," *IEEE Trans. Commun.*, vol. 59, no. 11, pp. 3122–3134, Nov. 2011.

[11] F. Gezer, R. G. Aykroyd, and S. Barber, "Statistical properties of poisson-voronoi tessellation cells in bounded regions," *J. of Statistical Computation and Simulation*, vol. 91, no. 5, pp. 915–933, 2021.

[12] 3GPP TR 38.901, "Technical Specification Group Radio Access Network; Study on channel model for frequencies from 0.5 to 100 GHz," 3rd Generation Partnership Project, Tech. Rep., 12 2023.